Optics & Laser Technology 158 (2023) 108795

Contents lists available at ScienceDirect

Optics and Laser Technology

journal homepage: www.elsevier.com/locate/optlastec

Full length article

Effects of anisotropic and isotropic LIPSS on polymer filling flow and wettability of micro injection molded parts

I. Gnilitskyi [a,b,c,*], W. Alnusirat [d], M. Sorgato [e], L. Orazi [f,g], G. Lucchetta [e,*]

[a] "NoviNano Lab" LLC, Lviv, Ukraine
[b] Department of Applied Physics and Nanomaterials Science, Lviv Polytechnic National University, Lviv, Ukraine
[c] INFN-Laboratori Nazionali di Frascati, Frascati, Italy
[d] Maan University College, Al-Balqa Applied University, Salt, Jordan
[e] University of Padova, Department of Industrial Engineering, Padova, Italy
[f] University of Modena and Reggio Emilia, Department of Science and Method for Engineering, Reggio Emilia, Italy
[g] EN&TECH, University of Modena and Reggio Emilia, Reggio Emilia, Italy

ARTICLE INFO

Keywords:
LIPSS
Injection molding
Hydrophobicity
Flow length

ABSTRACT

In micro injection molding, the specific cavity surface texture and roughness directly influence the polymer flow and the heat transfer between polymer melt and mold. In this work, two different types of laser-induced periodic surface structures, linear and hexagonal, were generated, and their impact on the flow length in micro injection molding was evaluated.

A complete investigation of the surface treatment effect on the polymer flow was carried out, comparing the performance of an untreated cavity surface with surfaces modified by LIPSS. The phenomenon was examined by localizing the weld lines created by the polymer flowing in two parallel channels having different surface treatments. Several cavity inserts were treated by varying the LIPSS process parameters to generate surfaces with different micro- and nanostructures directions and periodicity. Furthermore, the paper addresses the hydrophobicity achieved on the micro molded surfaces replicated from mold inserts with different LIPSS-based surface topography. Mold surfaces with linear and hexagonal LIPSS and the respective molded parts were analyzed by optical profilometry and scanning electron microscopy to characterize the cavity surfaces replication and localize the weld lines on the micro injection molded parts.

1. Introduction

Micro injection molding (μIM) of thermoplastic polymers is widely employed for the economical mass-production of micro surface geometries by replication, especially for optical and microfluidic applications. The complete replication of high aspect ratio micro features, usually placed on a relatively thick substrate, depends mainly on process conditions and polymer properties [1–2]. The melt polymer flow is laminar with a no-slip hydrodynamic boundary condition under regular injection velocity and cavity geometry in the conventional injection molding process. However, instabilities occur when geometry exhibits rapid changes, such as the presence of gates or thin sections, especially if combined with high-speed injection. The so-called wall slip is a well-known phenomenon for non-Newtonian fluids, which can be ascribed to the disentanglement of the bulk chains when attached to the mold walls [3–5]. This effect is more frequent in micro injection molding. Indeed, when downscaling the injection molding process, the rate between mold cavity surface and cavity volume increases, meaning that physical phenomena at the polymer-mold interface increase their relevance and influence on the whole process.

Using numerical tools to simulate and optimize a process is a well-consolidated approach in conventional injection molding, but commercial numerical codes fail to properly simulate the flow behavior and cavity filling when sizes are downscaled. Such inadequacy has to be ascribed to several limiting factors, but they all can be attributed to the fact that polymer rheological properties used in commercial simulation tools are obtained from macroscopic scale measurements. Conversely, surface tension and wall-slip conditions play a significant role within microscale geometries, depending on viscosity, heat transfer and temperature distribution, and the topography of cavity surface [6]. More

* Corresponding authors.
E-mail addresses: iaroslav.gnilitskyi@novinano.com (I. Gnilitskyi), walidnusir@bau.edu.jo (W. Alnusirat), leonardo.orazi@unimore.it (L. Orazi), giovanni.lucchetta@unipd.it (G. Lucchetta).

https://doi.org/10.1016/j.optlastec.2022.108795
Received 22 April 2022; Received in revised form 8 August 2022; Accepted 13 October 2022
Available online 4 November 2022

specifically, cavity surface topography, which in large-scale molding is relevant only for surface finishing and appearance, can significantly change the cavity volume at the micro-scale and influence the polymer flow and the heat transfer between polymer melt and mold [7].

The mold surface structure influences the melt flow behavior, and the molded parts' wettability is heavily affected by the cavity surface topography. Wettability is a fundamental property of solid surfaces governed by both the geometrical microstructure and the chemical composition of the surface. In recent years, superhydrophobicity, controllable water adhesion, anisotropic sliding, and anisotropic wetting, which are four specific aspects of wettability, have attracted much interest because of their importance in fundamental research, practical applications, and inspired mimetic attempts [8].

Modifying surface with femtosecond laser pulses is one-step, fast, chemically and vacuum-free technology compared to conventional methods, including coatings, chemical etching, and various lithography techniques [9,10]. The unique properties of femtosecond pulses are local treatment without overheating the modified material, well-defined ablation threshold with minimum thermal collateral damages [11]. A peculiar property of linearly polarized femtosecond laser pulses is the formation of self-organized structures, so-called Laser-Induced Periodic Surface Structures (LIPSS) [12,13]. LIPSS have been imprinted on almost all materials and demonstrated potential for many applications [12–17].

One of the applications of LIPSS based texturing is the surface modification of molds for polymer injection. An example can be found in [18,19], where authors investigated the effects of LIPSS orientation on polymer slip during PET injection molding with a significant reduction of injection pressure. However, only linear LIPSS have been investigated so far regarding their effect on injection mold filling. Hexagonal LIPSS, which were recently obtained using complicated beam interference schemes [20], have never been tested in this application. Therefore, their potential in facilitating cavity filling needs to be investigated.

In this work, two kinds of LIPSS were generated in a mold cavity, i.e. linear LIPSS and hexagonal LIPSS, to study their impact on the flow length during micro injection molding. In contrast to previous work [20], hexagonal LIPSS were obtained by using a simple optical path and an interpretation is offered to explain the formation of such hexagonal periodic structures. The effect of the surface treatments on the polymer flow was investigated by comparing the performance of an untreated cavity surface with treated ones. The phenomenon was analyzed using two parallel channels for melt separation and exploiting the localization of weld lines for differential characterization [21]. One channel was kept untreated on each sample, while the other was covered with LIPSS allowing a direct evaluation of the surface treatment benefits. Several cavity inserts were treated by varying the laser process parameters in order to generate LIPSS structures on the surfaces with different directions and periodicity to investigate a wide range of treatment solutions.

Furthermore, the hydrophobicity of the replicated LIPSS where characterized as hydrophobic surfaces are increasingly manufactured by creating submicron structures on plastic parts. Functionalities necessary for microfluidics, such as fluid collection or transport, may be made possible by the changed wetting behavior [22,23]. Surface replication and process characterization enable consistent production. It has been demonstrated that the creation of LIPSS using a femtosecond laser is an efficient method for functionalizing injection molding mold cavities. [24,19] The mold surface temperature was found by Krantz et al. to be the most important processing variable for precise and reliable surface replication for microinjection molded items. [25,18] Due to a reduction in melt viscosity at higher mold temperatures, the polymer melt may flow into the cavity more easily. The mold temperature must also be high enough to avoid the creation of a skin layer and the freezing off of the micro-structure prior to filling. Because of the decreased viscosity, raising the mold temperature also lowers the needed injection pressure and speed.

2. Experimental

2.1. Material and cavity design

Polystyrene (Total, PS Crystal 1540) was used in the micro injection molding experiments. The mold cavity was designed to analyze the specific effect of LIPSS surface treatments on wall slip and cavity filling. The proposed approach exploits a double channel with a double link configuration, as reported in Fig. 1.

The reference cavity is 15 mm long, 6 mm wide and 0.3 mm thick. The smaller hole is 1 mm wide and 1.5 mm long, while the longer one is 8 mm long. The cavity can be divided into four main sections. In the first one (p1 in Fig. 1), the channels are machined with the same width (2.5 mm), thickness (0.3 mm), and roughness. Consequently, when the split flows of molten polymer meet in the second section (p2), the weld line w1 is formed. Suppose any cause of asymmetries occurs, such as inaccurate machining of the cavity or uneven temperature distribution. In that case, the position of the weld line w1 in p2 will not be centered: the displacement can then be used to verify any presence of asymmetries within the cavity and to compensate it if any occurs. Therefore, the w1 location represents the 'zero-position' for the following analysis in section p4.

The third section (p3) is machined identically to the first one except for the surface topography, which is different between the two channels. As shown in Fig. 2, the LIPSS were realized only on the top channel of the cavity. Therefore, any filling flow difference between the two channels must be due to a different polymer-mold interaction caused by the LIPSS. If the polymer flowing in the treated channel accelerates (e.g. thanks to the reduced friction caused by the LIPSS) relative to that flowing in the untreated channel, the two flow fronts will not meet at the centerline. Therefore, such effect can be quantitatively evaluated in the fourth section (p4) as a relative y-direction displacement of the second weld line (w2) compared to w1.

2.2. Cavity surface treatments

The cavity surface treatments were performed using a Yb-based femtosecond laser system Pharos coupled with a galvo scanner and focused with a 56 mm f-theta lens. Two different types of LIPSS were carried out – linear LIPSS (treatment A) and hexagonal LIPSS (treatment B). As reported in Table 1, the laser source parameters were maintained constant except for the direction of the polarization plane and the use of argon shielding gas directed over the samples through a lateral nozzle.

2.3. Injection molding experiments

Injection molding experiments were carried out using a Wittmann-Battenfeld MicroPower 15 state-of-the-art micro injection molding machine (maximum injection speed: 750 mm/s, maximum clamping force: 150 kN). The machine has an injection system composed of a 14 mm plasticizing screw and a 5 mm injection plunger.

In order to investigate the surface treatments' influence on the flow behavior, an experimental plan was designed varying the injection speed within four levels: 30, 100, 300, and 750 mm/s. The same injection molding tests were carried out using an untreated mold insert as a reference.

2.4. Characterization of the molded parts

The weld lines locations were evaluated with a 3D optical profiler (Sensofar, PLu neox), used in confocal mode. The weld line distance from the edge of the treated side (D) was measured in five different positions along the x-axis, as shown in Fig. 2, and the average of these measurements was calculated. Five parts were characterized for each combination of injection velocity and mold insert treatment.

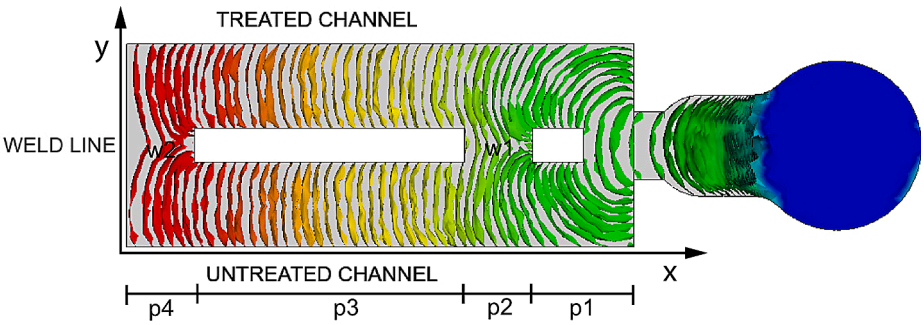

Fig. 1. The cavity design and the filling pattern, as predicted by a numerical simulation. The flow front advances from the right (blue) to the left (red), forming weld lines (w1 and w2) after the first and the second hole, respectively.

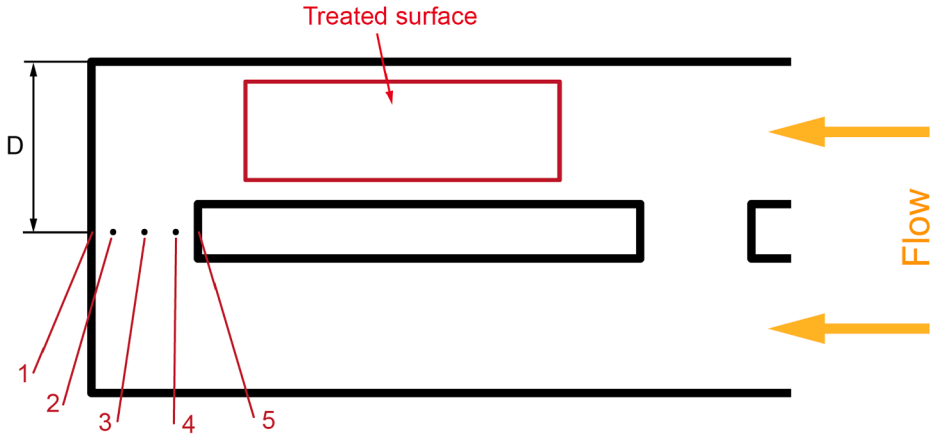

Fig. 2. LIPSS location in the cavity and measurement points along w2.

Table 1
Process parameters for the LIPSS treatments. The direction of the polarization plane was set parallel to the advancing flow front direction to generate nano-ripples oriented perpendicularly to the polymer flow.

Type of LIPSS	Linear	Hexagonal
Energy per pulse [nJ]	370	370
Pulse duration [fs]	120	120
Repetition Rate [MHz]	1	1
Step [μm]	4.5	4.5
Spot Diameter [μm]	10.4	10.4
Scanning Speed [mm/s]	1000	1000
Polarization direction respect to scanning direction	0°	90°
Shielding gas	Argon	In air

2.5. Wettability measurement

Furthermore, the molded parts were subjected to a dynamic wettability test with distilled-deionized water conducted through the sessile drop method. The tests were conducted on the LIPSS area by measuring the drops' contact angle variation with time for samples obtained by different mold and with different injection conditions.

The contact angle of laser-modified and non-modified surfaces was measured at room temperature (22 °C) using a Theta Flex optical tensiometer supplied by Biolin Scientific (Västra Frölunda, Sweden). The water contact angle of the samples was evaluated by static contact angle measurements, placing a 1 μL droplet of distilled water on the surface of the treated area. The image of the drop was then recorded for 10 s. An average value of contact angle was calculated based on at least five measurements. The static contact angle was then defined by fitting the Young-Laplace equation around the droplet.

2.6. FIB and SEM

The surface morphology was investigated by secondary electron imaging mode using an FEI Nova NanoSEM 450 with X-EDS Bruker QUANTAX-200. The cross-sectional sample was made on an FEI Scios Focused Ion beam (FIB)-SEM dual beam, and subsequently, EDS maps were obtained at 10 kV electron high voltage on an Oxford SDD energy dispersive X-ray spectrometer (EDS) attached to the FIB-SEM. To minimize the Ga beam damage to the LIPSS structure, care was taken by final polishing the cross-section using a small beam current (30 kV, 50 pA) before EDS maps and high-quality SEM images were taken.

3. Results and discussion

SEM analyses of the treated surfaces are presented in Fig. 3. The LIPSS shown in Fig. 3A, which is induced by linear polarized femtosecond laser pulses, is highly regular. The linear LIPSS appears due to the interference between the incident light and surface plasmons [12]. According to the hydrodynamic theories, especially influence hydrodynamic instabilities [26], we suppose that structures on Fig. 3B, where clearly visible hexagons, is the case of such hydrodynamic instability. It is known that smooth surface of the ferrofluids leads to lose of the stability in external magnetic fields and undergoes the Rosensweig instability if the applied field is larger than the critical value [27]. This instability manifests itself in the form of hexagonal arrangement over the localized structures, which grows from ferrofluid in the direction of the applied magnetic field. In the given images, the direction of the polymer filling flow will be horizontal.

SEM images cannot provide indications of the surface topography. Therefore, FIB cross-sections were created to measure the actual height of the ripples and valleys, as shown in Fig. 4 for linear (Fig. 4A) and

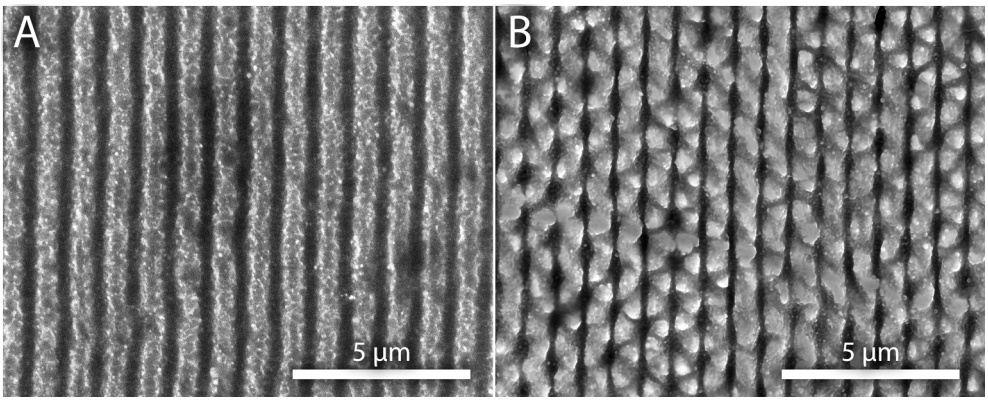

Fig. 3. LIPSS treated mold surfaces: (A) linear LIPSS, and (B) hexagonal LIPSS.

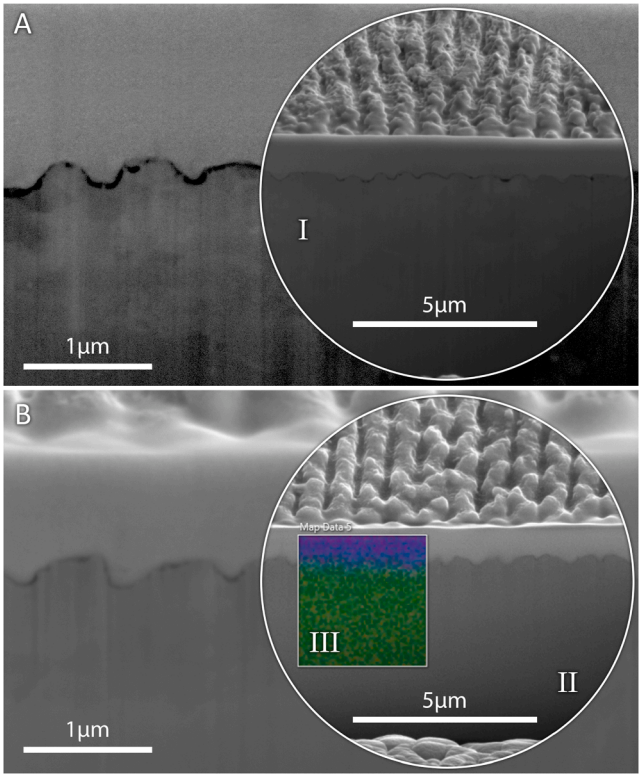

Fig. 4. SEM images of FIB sections of the mold surface LIPSS-treated in (A) linear and (B) hexagonal. Inset I depicts lower magnification of Fig. 4A. Insets II and III display lower magnification of Fig. 4B and EDS elements mapping after LIPSS treatment.

hexagonal LIPSS (Fig. 4B). The ripples thickness in bulk is around 300–350 nm for both modes. As shown by the EDS elements mapping Fe (green) is distributed equally in whole deep of the cross section and mixed with small particles of O_2 (orange).

Fig. 5 plots the weld line distance (*D*) averages for all the samples molded with the investigated treatment at different injection speeds.

The analysis of variance shows that the injection velocity significantly influences the weld line position for mold inserts treated with hexagonal LIPSS. Conversely, the injection velocity is not significant for mold inserts treated with linear LIPSS (p-value = 0.947).

For the injection speed of 30, 100, and 300 mm/s, there is a significant increase in the weld line distance (D) for mold inserts treated with hexagonal LIPSS compared with the untreated ones. However, no variations are visible for the specimens molded at 750 mm/s. Concerning the components molded with the mold insert treated with linear LIPSS, there is no evident variation between the calculated average position of the weld line compared with that one calculated for the specimens molded with the untreated mold insert.

The experimental results have shown that it is worth treating the mold cavity surface with hexagonal LIPSS in air to improve the filling behavior of a microcavity as long as the injection speed is kept at low values. This trend is not caused by the occurrence of wall slip since this phenomenon disappears at higher injection velocity while wall slip is expected to increase with injection speed [18,28,29]. Wall-slip velocity consistently increases with increasing wall shear stress, which is directly related to shear rate and thus flow rate. In fact, for higher values of the shear rate, the number of macromolecular disentangling from a monolayer of polymer chains adsorbed at the polymer-mold interface continuously increase, leading to higher slip velocity [30].

This polymer flow improvement is due to the better insulating effect of the hexagonal LIPSS, which decreases the melt heat loss to the mold and helps to keep its viscosity low [31,32]. This explanation is also in accordance with the negative influence of the injection speed on the cavity filling: the higher the injection speed, the higher the heat flow convected into the cavity, and the lower the effect of the thermal contact resistance.

The better insulating effect of the hexagonal LIPSS cannot be due only to the presence of an oxidation layer caused by treated the laser treating the surface in air. As it is clearly shown in Fig. 3, hexagonal LIPSS forms narrower and more closed pockets than the regular large trenches that characterize linear LIPSS. Air within the cavity, which is displaced by the advancing polymer flow front, is more easily trapped in the pockets of hexagonal LIPSS, thus reducing the contact surface area between polymer and mold and the associated heat transfer. A similar effect was reported by Surace et al. investigating the effect of cavity surface roughness on the filling flow in micro injection molding [33]. Higher values of cavity surface roughness, increased the amount of air trapped among the surface asperities causing a significant reduction in the melt cooling rate, thus causing a longer flow length.

The analysis of variance showed that both the parameter “Treatment” and “Injection speed” are significant. Fig. 6 shows the main effects, which reveal a decreasing weld line distance from hexagonal to linear LIPSS. On the other hand, the flow length shows a maximum in correspondence to the injection speed of 100 mm/s.

After the injection molding tests, the mold inserts surfaces were analyzed using an SEM. These measurements were carried out to detect any variation of the LIPSS. Fig. 7 shows the untreated surface cavity (left) and the treated surface in air (right). It is possible to see a high sticking phenomenon occurring on surfaces treated in air by comparing the images, and such a sticking phenomenon is not visible analyzing the surfaces treated with the use of argon shielding flow (Fig. 8).

The sticking phenomenon, seen on the cavity surface treated in air, is

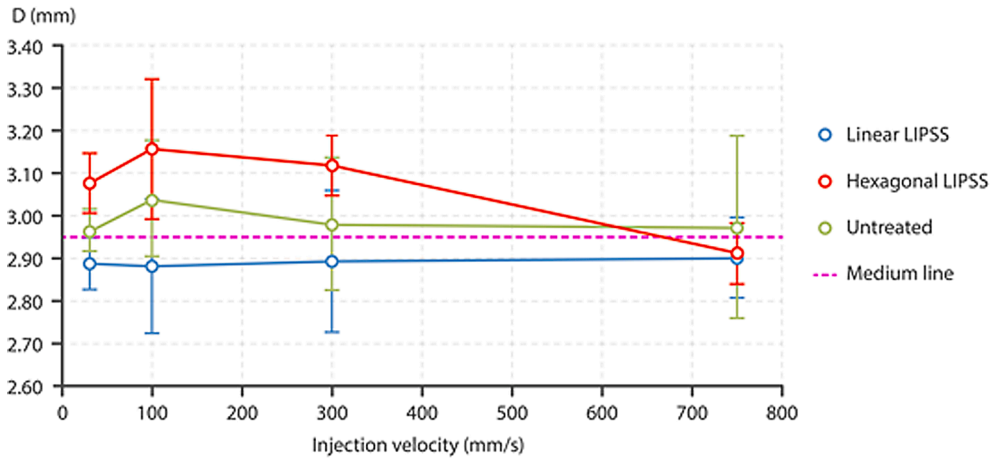

Fig. 5. Weld lines distance from the specimen edges on the treated side.

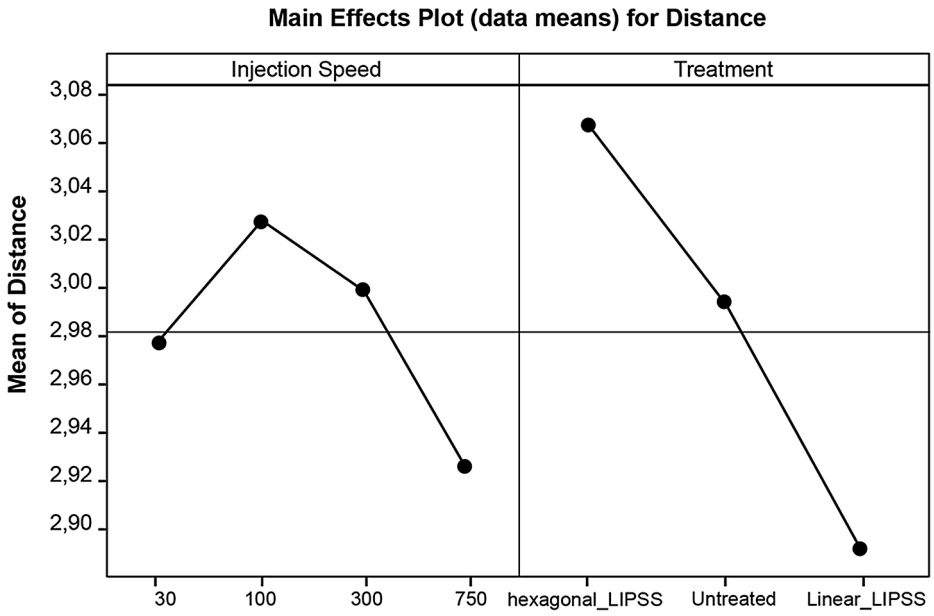

Fig. 6. Main effects plots.

due to a chemical adhesion between the polymer material and the oxidation layer, which develops in this process condition.

Fig. 9 shows the wettability test results for specimens obtained at two different injection speeds. Each test is the average value of 4 different repetitions, while the colored bands represent the amplitude of the standard deviation. Parts molded at low injection speed (30 mm/s) are more hydrophobic if textured with hexagonal LIPSS. The average contact angle is 15° and 30° lower for linear LIPSS and untreated parts, respectively. The lower hydrophobicity of linear LIPSS compared with hexagonal LIPSS can be explained considering the insulating effect of the latter, which allows for maintaining the polymer viscosity low thus favoring the replication of the LIPSS structures.

Increasing the injection velocity has been observed to increase replication of micro structured surfaces, as the cavity is filled before the skin layer solidifies, avoiding the microstructures freezing off prior to filling [34]. Moreover, molding at high injection speed causes the rapid compression of the air ahead of the flow front, which significantly increases the temperature of the flow front and favors the microstructures replication, as shown by Sorgato et al. [35]. This explains why at high injection speed the hydrophobicity of the linear LIPSS increases. A similar improvement observed for the untreated surface may be due to the better replication of a mold surface topography characterized by both micro and nanostructures, tightly packed. In fact, Liparoti et al. observed how in injection molding the hydrophobicity of the molded part can be increased by improving the replication of a low roughness cavity surface [36].

4. Conclusions

The analysis of variance showed that the hexagonal LIPSS was not influential on the filling flow length. Conversely, the linear LIPSS increase the filling behavior of the melt flow for injection speed up to 300 mm/s. For a higher injection speed, the surface treatment effect becomes negligible. The experimental tests have demonstrated that the injection speed of 100 mm/s is the optimal value to maximize the flow length. The SEM analysis of the surfaces treated in mode of linear LIPSS revealed a high attitude of the treatment to stick with the melt polymer.

On the contrary, this phenomenon does not occur with the treatment with hexagonal LIPSS. These results support the theory that the improvement of the polymer flow is not due to wall slip, and instead, it is caused by lower heat exchange between the melt and the oxidized mold surface.

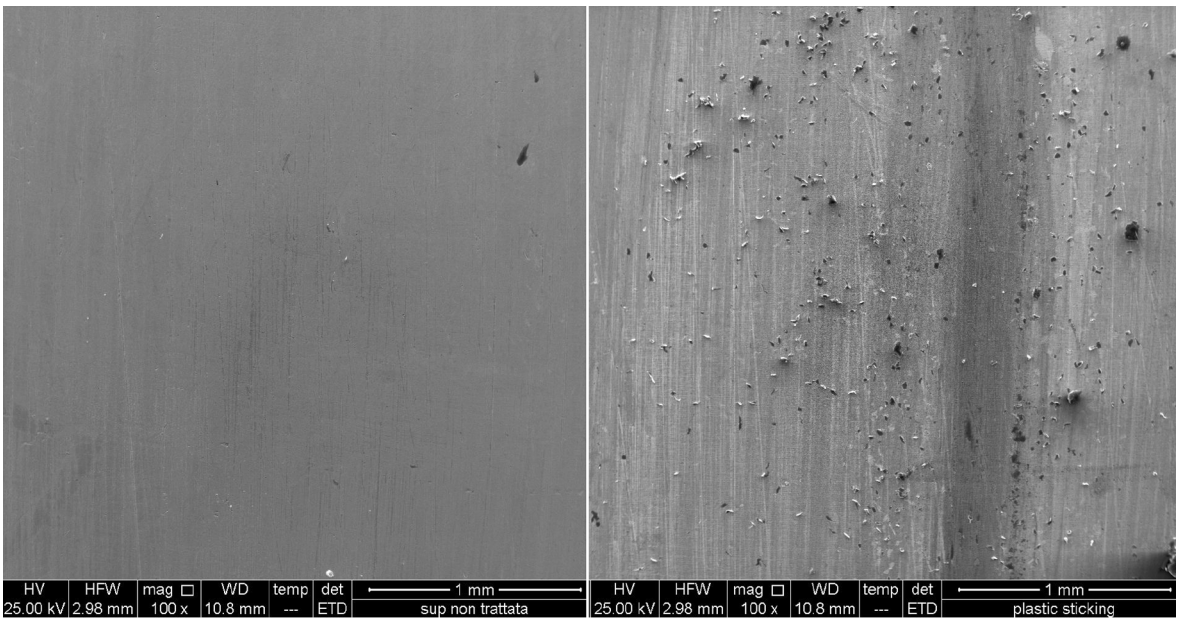

Fig. 7. Sticking of polymer material on the mold insert surface treated with hexagonal LIPSS (in air) on the right; untreated surface on the left (magnification: 100×).

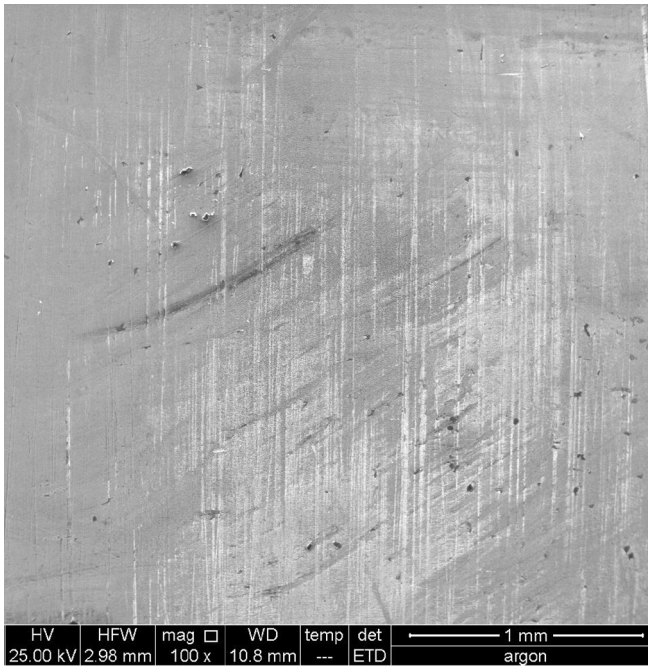

Fig. 8. Surface of the mold insert treated with linear LIPSS (under argon shielding flow) as analyzed after injection molding (magnification: 100×).

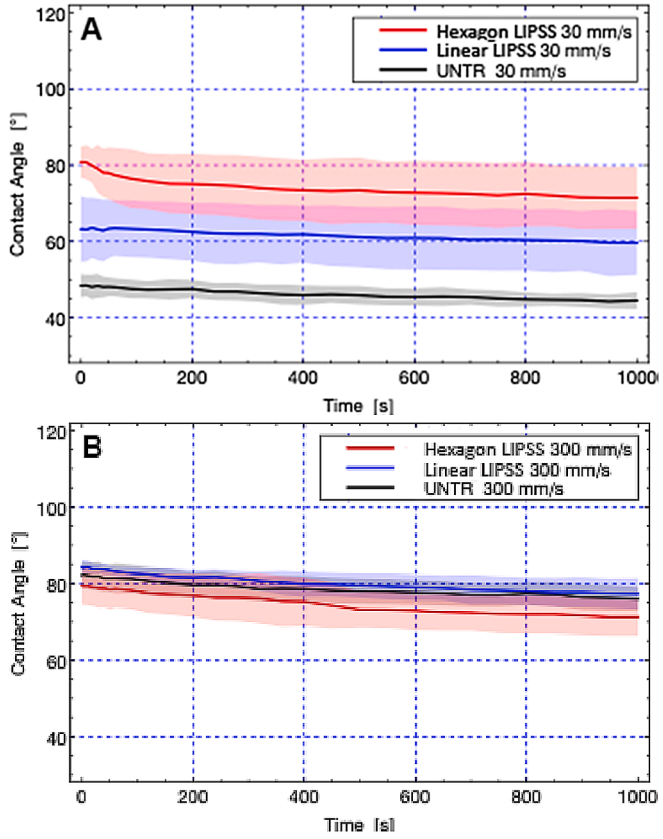

Fig. 9. Effects of LIPSS treatment on the dynamic wettability at various speed of polymer flow: 30 mm/s (A) and 300 mm/s (B).

CRediT authorship contribution statement

I. Gnilitskyi: Conceptualization, Methodology, Formal analysis, Investigation, Resources, Writing – original draft, Writing – review & editing, Visualization, Supervision, Project administration, Funding acquisition. **W. Alnusirat:** Methodology, Writing – review & editing. **M. Sorgato:** Methodology, Formal analysis, Investigation, Writing – review & editing. **L. Orazi:** Validation, Resources, Writing – review & editing, Supervision, Project administration, Funding acquisition. **G. Lucchetta:** Conceptualization, Validation, Formal analysis, Investigation, Resources, Writing – original draft, Writing – review & editing, Visualization, Supervision, Project administration, Funding acquisition.

Declaration of Competing Interest

The authors declare that they have no known competing financial interests or personal relationships that could have appeared to influence the work reported in this paper.

Data availability

Data will be made available on request.

References

[1] G. Tosello, A. Gava, H.N. Hansen, G. Lucchetta, F. Marinello, Characterization and analysis of weld lines on micro injection moulded parts using Atomic Force Microscope, Wear 266 (2009) 534–538, https://doi.org/10.1016/j.wear.2008.04.077.

[2] J. Zhao, X. Lu, M.S. Lin, G. Chen, S.L. Liu, M.S. Yong, Effects of rheological properties of polymer blends on micro mold filling behavior, Mater. Res. Innovations 10 (2006) 111–112.

[3] B. Sha, S. Dimov, C. Griffiths, M.S. Packianather, Micro-injection moulding: Factors affecting the achievable aspect ratios, Int. J. Adv. Manuf. Technol. 33 (2007) 147–156, https://doi.org/10.1007/s00170-006-0579-2.

[4] K.M. Awati, Y. Park, E. Weisser, M.E. Mackay, Wall slip and shear stresses of polymer melts at high shear rates without pressure and viscous heating effects, J. Non-Newtonian Fluid Mech. 89 (2000) 117–131, https://doi.org/10.1016/S0377-0257(99)00037-3.

[5] K. Komuro, K. Kobayashi, T. Taniguchi, M. Sugimoto, K. Koyama, Wall slip and melt-fracture of polystyrene melts in capillary flow, Polymer 51 (2010) 2221–2228, https://doi.org/10.1016/j.polymer.2010.03.014.

[6] M. Otsuka, A. Oyabe, H. Ito, Effects of mold surface conditions on flow length in injection molding process, Polym. Eng. Sci. 51 (7) (2011) 1383–1388, https://doi.org/10.1002/pen.21931.

[7] M. Burgesteiner, F. Müller, T. Lucyshyn, C. Kukla, C. Holzer, D. Gruber, J. Macher, G. Pacher, Investigation of the influence of different coatings on the filling behavior and replication quality of microstructures in injection molding, Proceedings of Polymer Processing Society 30th Annual Meeting PPS-30 July 8-12, 2014, Cleveland, Ohio (USA), 1-1 (2014).

[8] J. Yong, Q. Yang, F. Chen, D. Zhang, U. Farooq, G. Du, X. Hou, A simple way to achieve superhydrophobicity, controllable water adhesion, anisotropic sliding, and anisotropic wetting based on femtosecond-laser-induced line-patterned surfaces, J. Mater. Chem. 2 (15) (2014) 5499–5507.

[9] X. Liu, D. Du, G. Mourou, Laser ablation and micromachining with ultrashort laser pulses, IEEE J. Quantum Electron. 33 (10) (1997) 1706–1716, https://doi.org/10.1109/3.631270.

[10] B.N. Chichkov, C. Momma, S. Nolte, F. Von Alvensleben, A. Tünnermann, Femtosecond, picosecond and nanosecond laser ablation of solids, Appl. Phys. A 63 (2) (1996) 109–115, https://doi.org/10.1007/BF01567637.

[11] P. Balling, J. Schou, Femtosecond-laser ablation dynamics of dielectrics: basics and applications for thin films, Rep. Prog. Phys. 76 (3) (2013), 036502, https://doi.org/10.1088/0034-4885/76/3/036502.

[12] T. Apostolova, B. Obreshkov, I. Gnilitskyi, Ultrafast energy absorption and photoexcitation of bulk plasmon in crystalline silicon subjected to intense near-infrared ultrashort laser pulses, Appl. Surface Sci. 519 (2020), https://doi.org/10.1016/j.apsusc.2020.146087.

[13] J.Z.P. Skolski, G.R.B.E. Römer, J.V. Obona, V. Ocelik, A.J. Huis in 't Veld, J.T. M. De Hosson, M., Laser-induced periodic surface structures: fingerprints of light localization, Physical Review B. 85 (7) (2012), 075320, https://doi.org/10.1103/PhysRevB.85.075320.

[14] O.V. Kuznietsov, G.D. Tsibidis, A.V. Demchishin, A.A. Demchishin, V. Babizhetskyy, I. Saldan, S. Bellucci, I. Gnilitskyi, Femtosecond laser-induced periodic surface structures on 2D Ti–Fe multilayer condensates, Nanomaterials-Basel 11 (2021) 316, https://doi.org/10.3390/nano11020316.

[15] J. Bonse, S. Gräf, Maxwell Meets Marangoni—A Review of Theories on Laser-Induced Periodic Surface Structures, Laser Photonics Rev. 14 (2020) 2000215, https://doi.org/10.1002/lpor.202000215.

[16] I. Gnilitskyi, S. Mamykin, C. Lanara, I. Hevko, M. Dusheyko, S. Bellucci, E. Stratakis, Nanostructuring for Diffraction Grating Based Surface Plasmon-Resonance Sensors, Nanomaterials-Basel 11 (3) (2021) 591, https://doi.org/10.3390/nano11030591.

[17] Y. Kotsiuba, I. Hevko, S. Bellucci, I. Gnilitskyi, Bitmap and vectorial hologram recording by using femtosecond laser pulses, Sci. Rep. 11 (1) (2021) 1–8, https://doi.org/10.1038/s41598-021-95665-5.

[18] M. Sorgato, D. Masato, G. Lucchetta, L. Orazi, Effect of different laser-induced periodic surface structures on polymer slip in PET injection moulding, CIRP Ann. 67 (1) (2018) 575–578, https://doi.org/10.1016/j.cirp.2018.04.102.

[19] L. Orazi, M. Sorgato, L. Piccolo, D. Masato, G. Lucchetta, Generation and Characterization of Laser Induced Periodic Surface Structures on Plastic Injection Molds, Lasers Manuf. Mater. Process. 7 (2) (2020) 207–221.

[20] F. Fraggelakis, G. Mincuzzi, J. Lopez, I. Manek-Hönninger, R. Kling, Controlling 2D laser nano structuring over large area with double femtosecond pulses, Appl. Surf. Sci. 470 (2019) 677–686, https://doi.org/10.1016/j.apsusc.2018.11.106.

[21] G. Tosello, A. Gava, H.N. Hansen, G. Lucchetta, Study of process parameters effect on the filling phase of micro-injection moulding using weld lines as flow markers, Int. J. Adv. Manuf. Technol. 47 (1-4) (2010) 81–97.

[22] L. Gao, T.J. McCarthy, X.i. Zhang, Wetting and Superhydrophobicity, Langmuir 25 (24) (2009) 14100–14104.

[23] G. Mistura, M. Pierno, Drop mobility on chemically heterogeneous and lubricant-impregnated surfaces, Adv. Phys.: X. 2 (3) (2017) 591.

[24] A.-M. Kietzig, M. Negar Mirvakili, S. Kamal, P. Englezos, S.G. Hatzikiriakos, Laser-patterned super-hydrophobic pure metallic substrates: Cassie to Wenzel wetting transitions, J. Adhes. Sci. Technol. 25 (20) (2011) 2789–2809.

[25] J. Krantz, A. Caiado, L. Piccolo, P. Gao, M. Sorgato, G. Lucchetta, D. Masato, Dynamic wetting characteristics of submicron-structured injection molded parts, Polym. Eng. Sci. 62 (2022) 2093–2101.

[26] J. Reif, O. Varlamova, S. Varlamov, M. Bestehorn, Appl. Phys. A 104 (2011) 969.

[27] R. Rosensweig, Ferrohydrodynamics Ch. 7.1, Cambridge Univ. Press, 1985.

[28] D. Masato, M. Sorgato, M. Babenko, B. Whiteside, G. Lucchetta, Thin-wall injection molding of polystyrene parts with coated and uncoated cavities, Mater. Des. 141 (2018) 286–295, https://doi.org/10.1016/j.matdes.2017.12.048.

[29] D. Masato, M. Sorgato, A. Batal, S. Dimov, G. Lucchetta, Thin-wall injection molding of polypropylene using molds with different laser-induced periodic surface structures, Polym. Eng. Sci. 59 (9) (2019) 1889–1896, https://doi.org/10.1002/pen.25189.

[30] M. Ebrahimi, V.K. Konaganti, S. Moradi, A.K. Doufas, S.G. Hatzikiriakos, Slip of polymer melts over micro/nano-patterned metallic surfaces, Soft Matter 12 (48) (2016) 9759–9768.

[31] G. Lucchetta, D. Masato, M. Sorgato, L. Crema, E. Savio, Effects of different mould coatings on polymer filling flow in thin-wall injection moulding, CIRP Ann. 65 (1) (2016) 537–540, https://doi.org/10.1016/j.cirp.2016.04.006.

[32] M. Sorgato, D. Masato, L. Piccolo, G. Lucchetta, Plastic intensity reduction using thermally insulating coatings for injection molds, CIRP J. Manuf. Sci. Technol. 30 (2020) 79–86, https://doi.org/10.1016/j.cirpj.2020.04.004.

[33] R. Surace, M. Sorgato, V. Bellantone, F. Modica, G. Lucchetta, I. Fassi, Effect of cavity surface roughness and wettability on the filling flow in micro injection molding, J. Manuf. Process. 43 (2019) 105–111, https://doi.org/10.1016/j.jmapro.2019.04.032.

[34] D. Masato, M. Sorgato, G. Lucchetta, Analysis of the influence of part thickness on the replication of micro-structured surfaces by injection molding, Mater. Des. 95 (2016) 219.

[35] M. Sorgato, M. Babenko, G. Lucchetta, B. Whiteside, Investigation of the influence of vacuum venting on mould surface temperature in micro injection moulding, Int. J. Adv. Manuf. Technol. 88 (1-4) (2017) 547–555.

[36] S. Liparoti, R. Pantani, A. Sorrentino, V. Speranza, G. Titomanlio, Hydrophobicity Tuning by the Fast Evolution of Mold Temperature during Injection Molding, Polymers. 10 (2018) 322.